Pt and Sn doped sputtered CeO2 catalysts for fuel cell applications

Vladimir Matolin, Milos Cabala, Iva Matolinova, Michal Skoda, Michal Vaclavu, Tomas Skala, Kevin Charles Prince, Toshiyuki Mori, Heideki Yoshikawa, Y Yamashita, et al.

Pt and Sn doped sputtered CeO2 catalysts for fuel cell applications

Journal:	*Fuel Cells*
Manuscript ID:	fuce.200900036.R2
Wiley - Manuscript type:	Original Research Paper
Date Submitted by the Author:	13-Nov-2009
Complete List of Authors:	Matolin, Vladimir; Charles University, Surface and Plasma Science Cabala, Milos; Charles University, Surface and Plasma Science Matolinova, Iva; Charles University, Surface and Plasma Science Skoda, Michal; Charles University, Surface and Plasma Science Vaclavu, Michal; Charles University, Surface and Plasma Science Skala, Tomas; Sincrotrone Elettra, MSB Prince, Kevin; Sincrotrone Elettra, MSB Mori, Toshiyuki; NIMS, Fuel Cell Yoshikawa, Heideki; National Institute for Materials Science, SPring-8 Yamashita, Y; National Institute for Materials Science, SPring-8 Ueda, S; National Institute for Materials Science, SPring-8 Kobayashi, K; National Institute for Materials Science, SPring-8
Keywords:	Fuel Cell Electrode, Oxide Thin Films, PEM Fuel Cell, Platinum, X-ray Photoelectron Spectroscopy

DOI: 10.1002/adfm.((please add manuscript number))

Pt and Sn doped sputtered CeO_2 electrodes for fuel cell applications

V. Matolín*, M. Cabala, I. Matolínová, M. Škoda, M. Václavů, K.C. Prince, T. Skála, T. Mori, H. Yoshikawa, Y. Yamashita, S. Ueda, K. Kobayashi.

[*] *V. Matolín*, M. Cabala, I. Matolínová, M. Škoda, M. Václavů,*
Charles University, Faculty of Mathematics and Physics, Department of Surface and Plasma Science
V Holešovičkách 2, 18000 Prague 8, Czech Republic
e-mail: matolin@mbox.troja.mff.cuni.cz

K.C. Prince, T. Skála
Sincrotrone Trieste,
Strada Statale 14, km 163.5, 34012 Basovizza-Trieste, Italy

T. Mori
Ecomaterials Center, National Institute for Material Science,
Namiki, Tsukuba, 305-0044, Japan

H. Yoshikawa[4], Y. Yamashita[4], S. Ueda[4], K. Kobayashi[4]
National Institute for Materials Science, SPring-8,
Sayo-cho, Sayo, Hyogo 679-5148, Japan

[**] ((Acknowledgements, general annotations, funding.))

Keywords:
photoelectron spectroscopy, synchrotron radiation, cerium oxide, Pt, fuel cell

Abstract

The interaction of Pt with CeO_2 layers was investigated by using photoelectron spectroscopy. 30 nm thick Pt and Sn doped CeO_2 layers were deposited simultaneously by rf-magnetron sputtering on a Si(001) substrate and a carbon diffusion layer of a polymer membrane fuel cell by using a composite CeO_2-Pt-Sn target. The laboratory XPS and synchrotron radiation soft X-ray and hard X-ray photoemission spectra showed the formation of cerium oxide with completely ionized $Pt^{2+,\ 4+}$ species, and with Pt^{4+} embedded in the film bulk. Hydrogen/air fuel cell activity measurements normalized to the

amount of Pt used revealed high specific power of up to 5.4 x 10^4 mW/mg(Pt). The activity of these materials is explained by the strong activity of embedded Pt^{n+} cations.

1. Introduction

Pt - cerium oxide systems have been reported to be significantly active catalysts for CO oxidation[1], hydrogen production[2], oxidation of ethanol[3] and decomposition of methanol[4]. High activity for the water gas shift reaction was predicated on the presence of cationic platinum[5,6] in cerium oxide. Pt-oxide materials such as Pt-RuO_2[7] or Pt-SnO_2[8] and Pt-CeO_2[9-13] have been reported as promising anode materials for polymer membrane fuel cells (PMFC). Furthermore, the addition of Sn has an important effect on the electronic structure of Pt and its adsorption and reaction properties[3, 14- 20].

There are many photoelectron spectroscopy data showing different 4f configurations in ceria by using Ce 3d spectra[21-23]. Interaction of ceria with hydrogen leads to higher concentration of Ce^{3+} ions due to surface reduction[23], i.e. creation of oxygen vacancies.

Studies of the deposition of CeO_2 films using the rf-sputtering method were published in the past, e.g. [24,25]. In this study we report simultaneous magnetron sputtering of platinum, tin and cerium oxide which provides oxide layers continuously doped with Pt and Sn atoms during the film growth. We show that Pt doped cerium oxide films exhibit an unusually high concentration of cationic platinum Pt^{2+} and Pt^{4+} (nearly 100%) which opens the way for using such systems as highly active thin film catalysts. The addition of Sn causes cerium oxide reduction $Ce^{4+} \rightarrow Ce^{3+}$ and the formation of a Pt-Sn-Ce mixed oxide. When used as an anode material in hydrogen PMFC, Pt embedded in sputtered ceria films exhibits very high specific power (W/mg Pt) showing that such material represents a promising alternative catalyst for FC applications[26].

2. Results

Fuel cell

Non-reactive radio frequency (RF) magnetron sputtering was used to deposit CeO_2, Pt-CeO_2 and Pt-Sn-CeO_2 thin films on microporous gas diffusion layer (GDL, Alfa Aesar, Toray carbon paper, teflonated, TGP-60). CeO_2 sputtering was performed by using a 2" CeO_2 target at a distance of 90 mm from the substrate with rf power of 80 W, giving a growth rate of the cerium oxide films of 1 nm/min. The Pt-CeO_2 and Pt-Sn-CeO_2 thin films were deposited from the composite target prepared by placing pieces of 0.5 mm thick and 10 mm long Pt and Sn wires on the ceria target surface in the radial direction. Deposition was carried out at room temperature of the substrate in an Ar atmosphere by keeping constant the total pressure in the deposition chamber at 6×10^{-3} mbar.

Fuel cell tests were performed by using a specially designed small polymer membrane fuel cell device[26] at room temperature. The pretreatment of Nafion 0.09 mm membranes was performed by using a standard process of boiling in H_2O_2 solution, dilute H_2SO_4 and H_2O[27]. The cathode electrodes were made by carbon-supported Pt powder (Alfa Aesar, Platinum, nominally 40% on carbon black) mixed with the Nafion solution (Alfa Aesar, Perfluorosulfonic acid-PTFE copolymer, 5% w/w solution) and coated on the microporous GDL. The loading of Pt in the cathode catalyst layer was 5 mg/cm^2.

The anode GDL was coated with 30 nm thick Pt and Pt-Sn doped sputtered films. The pretreated Nafion membrane was sandwiched by the catalyzed anode and cathode by hot-pressing to form MEA of 1 cm^2 (10 x 10 mm).

To evaluate cell performance pure humidified hydrogen and air were used as fuel and oxidant at atmospheric pressure. The flow rates of H_2 and O_2 were controlled at 30.0 ml/min. The performance of the fuel cell with sputtered anode was compared with that of the reference FC. The reference FC differed from the tested one by the anode preparation only. The reference FC anode was made by using standard Pt-Ru powder catalysts (Alfa Aesar, Pt50, Ru50 at.%) mixed with Nafion solution and spread over the GDL surface with a loading of 5mg/cm^2.

The XRD pattern (not shown) of Pt doped ceria film shows only diffraction features which can be associated with CeO_2. The average ceria grain size, determined from the Debye-Scherrer formula from the (220)CeO_2 pattern, is 4.4 nm.

Pt-(Sn)-CeO_2 film thickness and surface morphology were determined by means of scanning electron microscopy (SEM) by using a TESCAN - MIRA microscope at 20 keV electron beam energy and atomic force microscopy (AFM, Veeco) in tapping mode. SEM (Fig. 1 a) and AFM (Fig 1 b) images of the Pt, Sn doped cerium oxide reference film show typical morphology of the layer surface, which is similar for both Pt and Pt-Sn doped samples. The films exhibit average surface roughness of approximately 2 nm.

The layer thickness was for all samples 30 nm and it was controlled by means of the SEM cross-sectional view of the broken reference sample obtained by the simultaneous deposition on a Si(001) wafer. Example of the thickness control is shown in Fig. 2. The back-scattered electron SEM shows a bright image of the catalyst film (Pt-CeO_2 in this case), figure inset shows corresponding chemical analysis obtained by the energy dispersive spectroscopy of x-rays (EDX). Performance of the miniaturized PMFC prepared by catalyzing the anode GDL with the above described rf sputtered Pt-CeO_2 and Pt-Sn-CeO_2 catalyst is shown in Figs. 3 a and 3 b, respectively. The Pt-CeO_2 anode gave a measured power density of 4.9 mW/cm^2 while the Pt-Sn-CeO_2 catalyst revealed an increase to 10.5 mW/cm^2.

Pt and Sn concentrations in Pt-CeO_2 and Pt-Sn-CeO_2 catalyst relative to the number of Ce atoms were determined by quantitative XPS (the spectra are not shown) using Ce 3d, Sn 3d and Pt 4f peak areas and XPS sensitivity factors. The concentrations were 7 at% of Pt for Pt-CeO_2 and 7 at% of Pt and 8 at% of Sn for the Pt-Sn-CeO_2 catalyst film. The Pt concentration determined in this way corresponded to an average Pt concentration in the approximately 2 nm thick surface layer probed by XPS (hν=1486 eV). Concentration in weight percent of Pt in the anode catalyst was calculated from the Pt-CeO_2 film thickness (30 nm) and Pt atomic concentration, and gave values of 2.2×10^{-3} mg of Pt per cm^2 of the anode. This made it possible to calculate maximum specific power SP_{max} for the both catalysts. For Pt-

CeO_2 and Pt-Sn-CeO_2 films, we found SP_{max}= 2.5 and 5.4 W/mg(Pt), respectively. In comparison with the SP_{max} value obtained for the standard Pt-Ru anode (SP_{max} = 0.04 W/mg(Pt)[26]), both sputtered catalysts exhibited very high activity per unit Pt content.

Photoelectron spectroscopy

The photoemission spectroscopy of Si supported reference samples was performed with X-rays of three different energies in order to vary the kinetic energy of the photoelectrons, and therefore the probing depth. We refer here to the lowest energy as soft X-ray photoelectron spectroscopy (SX-PES). These measurements were performed in an ultrahigh vacuum chamber of the experimental system at the Materials Science Beamline (MSB) at the Elettra synchrotron light source in Trieste ($h\nu$ = 180 eV, ΔE = 200 meV). The highest energy photoemission spectra referred as hard x-ray photoelectron spectroscopy (HX-PES) were performed at BL15XU beamline of the SPring8 synchrotron facility[28]. The total energy resolution ΔE = 280 meV was determined from the Fermi edge of an Au reference sample. Medium energy photoelectron spectra were measured using an Al X-ray source ($h\nu$ = 1486.6 eV, ΔE = 1 eV) and we refer to these data simply as XPS results. All PES experiments were performed ex situ in ultra-high vacuum (UHV) experimental chambers operating at base pressures < 10^{-10} mbar. The SX and HX-PES spectra were taken at normal emission, while XPS was measured at two photoelectron emission angles 20° and 60° with respect to the surface normal, in order to change surface sensitivity.

The high resolution 3d core level HX-PES (5946.8 eV) spectrum of the CeO_2 film deposited on Si(001) without adding Pt is presented in Fig. 4 (bottom curve). It consists of three $3d_{3/2}$-$3d_{5/2}$ spin-orbit-split doublets characteristic of stoichiometric CeO_2 (Ce^{4+}). The doublets represent different 4f configurations in the photoemission final state and arise from the Ce 4f hybridization in both the initial and the final states. The middle curve in Fig. 4 shows a HX-PES Ce 3d spectrum obtained for Pt doped films. The spectra CeO_2 and Pt-CeO_2 films are identical, showing that there is no measurable influence of added platinum on the cerium oxide stoichiometry.

The Pt 4f PES spectra obtained for the Pt doped ceria films are plotted in Fig. 5. Spectra at different photon energies have different information depth. For HX-PES the kinetic energy of the Pt 4f electrons is about 5870 eV corresponding to an inelastic mean free path in CeO_2 of λ = 7 nm [29]. For hν = 180 eV, the kinetic energy of the Pt 4f photoelectrons is close to 110 eV, corresponding to λ of 0.5 nm.

The spectrum at hν = 180 eV has the highest surface sensitivity. It exhibits a Pt $4f_{5/2}$ - $4f_{7/2}$ doublet at 72.9 eV corresponding to Pt^{2+} [6] and a doublet shifted by 1.4 eV to higher binding energy (BE) corresponding to Pt^{4+} [3]. A small peak at 71.8 eV is assigned to the Pt^0 state. This energy is slightly higher than that expected for metallic platinum. This shift can be explained, however, by a size effect in PES, which is generally observed for very small particles (below 2 nm). The ratio of the Pt^0 peak area relative to the whole Pt signal Pt^0/Pt = 0.035. Fig. 5 clearly shows that with increasing hν, the relative intensity of Pt^{4+} increases. The relative concentrations of Pt^{4+} and Pt^{2+} are presented in Table 1

The upper curve in Fig. 5 shows the Pt 4f HX-PES spectrum obtained for the Pt doped ceria film, i.e. the spectrum measured at highest information depth. The spectrum exhibits Pt $4f_{7/5}$ – $4f_{5/2}$ doublets corresponding to Pt^{4+} and Pt^{2+} states only. Contribution of Pt^0 is negligible, which indicates that platinum atoms in the ceria layer are fully oxidized. The Pt 4f spectrum obtained by HX-PES reveals a platinum ion concentration ratio of Pt^{4+}/Pt^{2+} = 1.45.

The XPS Pt 4f spectra, middle and bottom, also show high intensity of the Pt^{2+} and Pt^{4+} with negligible Pt^0 signal. In order to change the surface sensitivity of XPS we measured the photoelectron emission for different angles of outgoing electrons relative to the surface normal. In Fig. 5 we compare spectra taken at 60° (λ = 1 nm) and 20° (λ = 2 nm)[29]. Pt 4f XPS spectra obtained for a photoelectron escape angle of 60° (higher surface sensitivity) and 20° (lower surface sensitivity) show Pt^{4+}/Pt^{2+} ratios of 0.77 and 1.06, respectively, i.e. angle resolved XPS confirms a substantial increase of the Pt^{4+} signal with decreasing surface sensitivity.

A simple estimation based on the enhancement of the Pt^{4+} signal as a function of λ leads to a structural model with very low concentration of metallic platinum on the surface, Pt^{2+} rich Pt-ceria interface and surface region, and Pt^{4+} dispersed in the ceria film bulk.

Fig. 6 shows Pt 4f spectra of the ceria layer simultaneously doped with Pt and Sn during the film growth. The upper spectrum was obtained for HX PES at hν = 5946 eV. We fitted the spectrum with two doublets, with the most intense peak corresponding to Pt^{2+}. The Pt^{4+} intensity observed in Fig. 5 at 74.3 eV vanished whilst a new state appeared at Pt $4f_{7/2}$ = 74.8 eV, indicating the formation of a new chemical state of Pt. The corresponding HX PES Ce 3d spectrum in Fig. 4 (upper curve) clearly indicates that tin induces a partial reduction of ceria which can be seen as appearance of the Ce^{3+} states in the film bulk. We calculated the Ce^{3+}/Ce^{4+} concentration ratio as the ratio of the sums of areas of the corresponding fits in Fig. 4, and obtained a value of Ce^{3+}/Ce^{4+} = 0.28, showing that approximately 25% of Ce atoms are in the Ce^{3+} state. The partial reduction of cerium oxide by tin is in agreement with our previous results showing a strong Sn-CeO_2(111) interaction leading to the $Ce^{4+} \rightarrow Ce^{3+}$ transition[18].

Fig. 7 presents the Sn $3d_{5/2}$ spectrum of the Pt-Sn-CeO_2/Si sample. The BE of the Sn $3d_{5/2}$ state of 486.7 eV corresponds to Sn^{4+}.

The BE of Pt $4f_{7/2}$ in a Pt-Sn alloy is close to 71 eV [14, 15], i.e. it has a relatively small shift relative to metallic Pt. The high binding energy of Pt $4f_{7/2}$ observed in our case together with a Sn $3d_{5/2}$ BE typical for SnO_2 leads to the conclusion that the new Pt phase in the Pt-Sn-ceria film might correspond to a binary Pt-Sn and/or ternary Pt-Sn-Ce mixed species, probably highly dispersed in the catalyst film.

Similarly to the case of the Pt-CeO_2/Si sample we changed the information depth of the analysis by taking spectra at different photon energies and different electron emission angle. The results in Fig. 6 show a decrease of the Pt-Sn phase (74.8 eV) concentration relative to Pt^{2+} with increasing surface sensitivity. The results are presented in Table 1.

Sn has an important chemical effect on the electronic structure of Pt, and in particular induces changes in the d- band occupation due to d – sp orbital hybridization, Pt → Sn charge transfer and an increase of the Pt 5d hole number[14]. Pt → Sn charge transfer is in agreement with the observed high binding

energy of the new platinum state. An increase of the Pt 5d hole number could tentatively explain the observed high activity of the Pt-Sn-CeO_2 anode in the hydrogen PMFC due to an increase of the probability of $H \rightarrow H^+ + e^-$ splitting.

3. Conclusion

The Pt and Pt-Sn doped CeO_2 polycrystalline films prepared by rf sputtering exhibit excellent properties as anode material for hydrogen PMFC. Particularly the ceria films containing both Pt and Sn cations exhibit very high specific power (power output expressed relative to 1 mg of Pt).

In the case of the Pt-CeO_2 film, Pt atoms buried in the bulk are completely ionized to form Pt^{4+} oxide species. We found that a small amount of Pt^0 was present on the film surface. The surface region probed by photoelectrons with an inelastic mean free path of 0.5 nm exhibits mainly Pt^{2+} states. We conclude that the surface region contains Pt^{2+} species whilst the film bulk contains dispersed Pt^{4+}. We believe that the high oxidation state of platinum inside the layer is due to the atomic dispersion of Pt resulting from the preparation method – co-sputtering of cerium oxide and Pt. Cerium oxide has especially Ce^{4+} character with concentration of eventual Ce^{3+} species under the detection limit of the present method.

The Pt-Sn-CeO_2 films differ from Pt-CeO_2 by partial reduction of the cerium oxide and formation of a new bulk chemical state of Pt in Pt-Sn-Ce mixed oxide. Pt → Sn charge transfer suggests strong Pt - Sn interaction, however we are not yet able to explain satisfactorily the chemical state of the new Pt phases in the sputtered ceria films. This work represents the first study of such materials prepared by using the process of non reactive rf sputtering, which leads to the preparation of materials having properties different from those prepared by common chemical processes (co-precipitation, impregnation, etc).

High activity of the Pt doped ceria films seems to be linked to a high dispersion of Pt in CeO_2 forming active $Pt^{4+,2+}$ species in the Pt(Sn)-Ce mixed oxide. The study, showing the possibility of controlled variation of Pt^{4+}/Pt^{2+} ratio as a function of deposition parameters and resulting impact on the reactivity, is in progress.

Acknowledgements

This work is a part of the research programs No. MSM 0021620834, ME08056 and LC06058 that are financed by the Ministry of Education of the Czech Republic.

References

[1] Y. Suchorski, R. Wrobel, S. Becker, B. Strzelczyk. W. Drachsel, H. Weiss, Surf. Sci. **2007**, 601, 4843.

[2] P. Y. Sheng, W. W. Chiu, A. Yee, S. J. Morrison, H. Idriss, Catal. Today **2007**, 129, 313.

[3] X. Tang, B. Zhang, Y. Li, Y. Xu, Q Xin, W. Shen, J. Mol. Catalysis A **2005**, 235, 122.

[4] S. Immamura, T. Higashihara, Y. Saito, H. Aritani, H. Kanai, Y. Matsumura, N. Tsuda, Catalysis Today **1990**, 50, 369.

[5] D. Pierre, W. Dong, M. Flytzani-Stephanopoulos, Top. Catal. **2007**, 46, 363.

[6] Q. Fu, H. Saltsburg, and M. Flytzani-Stephanopoulos, Science **2003**, 301, 935.

[7] A. Katayama, J. Phys. Chem. **1980**, 84, 376.

[8] P. K. Shen, A. C. C. Tseung, J. Electrochem. Soc. **1994**, 141, 3082.

[9] C. Xu, R. Zeng, P. K. Shen, Z. Wei, Electrochim. Acta **2005**, 51, 1031.

[10] C. L. Campos, C. Roldan, M. Aponte, Y. Ishikawa, C. R. Cabrera, J. Electroanal. Chem. **2005**, 581, 206.

[11] M.Takahashi, T.Mori, A.Vinu, H.Kobayashi, J.Drennan, D.-R.Ou, J. Mater. Res. Soc. **2006**, 21, 2314.

[12] M.Takahashi, T.Mori, F.Ye, A.Vinu, H.Kobayashi, J.Drennan, J. Am. Ceram. Soc. **2007**, 90, 1291.

[13] M. Takahashi, T. Mori, A. Vinu, D. R. Ou, H. Kobayashi, J. Drennan, Advances Appl. Ceramics **2007**, 57, 107.

[14] J. M. Ramallo-lopez, G. F. Santori, L. Giovanetti, M. L. Casella, O. A. Ferretti, F. G. Requejo, J. Phys. Chem. B **2003**, 107, 11441.

[15] E. Janin, M. Bjorkqvist, T.M. Grehk, M. Gothelid, C.-M. Pradier, U. O. Karlsson, A. Rosengren, Appl. Surf. Sci. **1996**, 99, 371.

[16] A. Sumer, A. E. Aksoylu, Surf. Sci. **2008**, 602, 1636.

[17] J. L. Margitfalvi, I. Borbath, K. Lazar, E. Tfirst, A. Szegedi, M. Hegedus, S. Gobolos, J. Catalysis **2001,** 94, 203.

[18] M. T. Paffet, S. C. Gebhard, R. G. Windham, B. E. Koel, J. Phys. Chem. **1990,** 94, 6831.

[19] G. Neri , G. Rizzo, A.S. Arico, C. Crisafulli, L. De Luca, A. Donato, M.G. Musolino, R. Pietropaolo, Applied Catalysis A: General **2007,** 15, 325.

[20] H. A. Gasteiger, N. M. Markovic, P. N. Ross Jr., J. Phys. Chem. **1995**, 99, 8945.

[21] S. H. Overbury, D. R. Mullins, D. R. Huntley, L. Kundakovic, J. Catal. **1999**, 186, 296.

[22] V. Matolín, M. Cabala, V. Cháb, I. Matolínová, K. C. Prince, M. Škoda, F. Šutara, T. Skála, K. Veltruská, Surf. Interf. Anal. **2008**, 40, 225.

[23] A. Pfau, K. D. Schierbaum, Surf. Sci. **1994**, 71, 321.

[24] M. Španková, I. Vávra, Š. Gaži, D. Machajdík, Š . Chromík, K. Fröhlich, L. Hellemans, Š. Beňačka, J. Crystal Growth **2000**, 218, 287.

[25] I. Iordanova, L. Popova, P. Aleksandrova, G. Beshkov, E. Vlahkov, R. Mirchev, B. Blagoev, Thin. Sol. Films **2007**, 515, 8078.

[26] M. Václavů, I. Matolínová, J. Mysliveček, R. Fiala, V. Matolín, J. Electrochem. Soc., **2009**, 156, B938.

[27] G.Q. Lua, C.Y. Wang, T.J. Yen, X. Zhang, Electrochim. Acta **2004**, 49, 821.

[28] K. Kobayashi, M. Yabashi, Y. Takata, T. Tokushima, S. Shin, K. Tamasaku, D. Miwa, T. Ishikawa, H. Nohira, T. Hattori, Y. Sugita, O. Nakatsuka, A. Sakai, S.Zaima, Appl. Phys. Lett. **2003**, 83, 1005.

[29] S. Tanuma, C.J. Powell, D.R. Penn, Surf. Interf. Anal. **1993**, 21, 165.

Figure captions

Figure 1.

Image of the magnetron sputtered Pt-Sn-cerium oxide film: (a) SEM, (b)AFM

Figure 2.

Cross-sectional SEM and EDX image of the Pt-CeO_2/Si catalyst film.

Figure 3.

Polarization and power density vs. current density using hydrogen/air flow at room temperature. FC with (a) Pt-CeO2 anode, (b) Pt-Sn-CeO2 anode

Figure 4.

Ce 3d HX PES spectra (hν = 5946.8 eV) of the rf magnetron sputtered films. Bottom spectrum was measured on pure cerium oxide film, upper spectra on Pt and Pt-Sn doped samples.

Figure 5.

The SX, XPS at photoemission angle of 20° and 60°, and HX Pt 4f spectra of the Pt-CeO_2 film.

Figure 6.

The SX, XPS at photoemission angle of 20° and 60°, and HX Pt 4f spectra of the Pt-Sn-CeO_2 film.

Figure 7.

The HX Sn $3d_{5/2}$ spectra of the Pt-Sn-CeO_2 film.

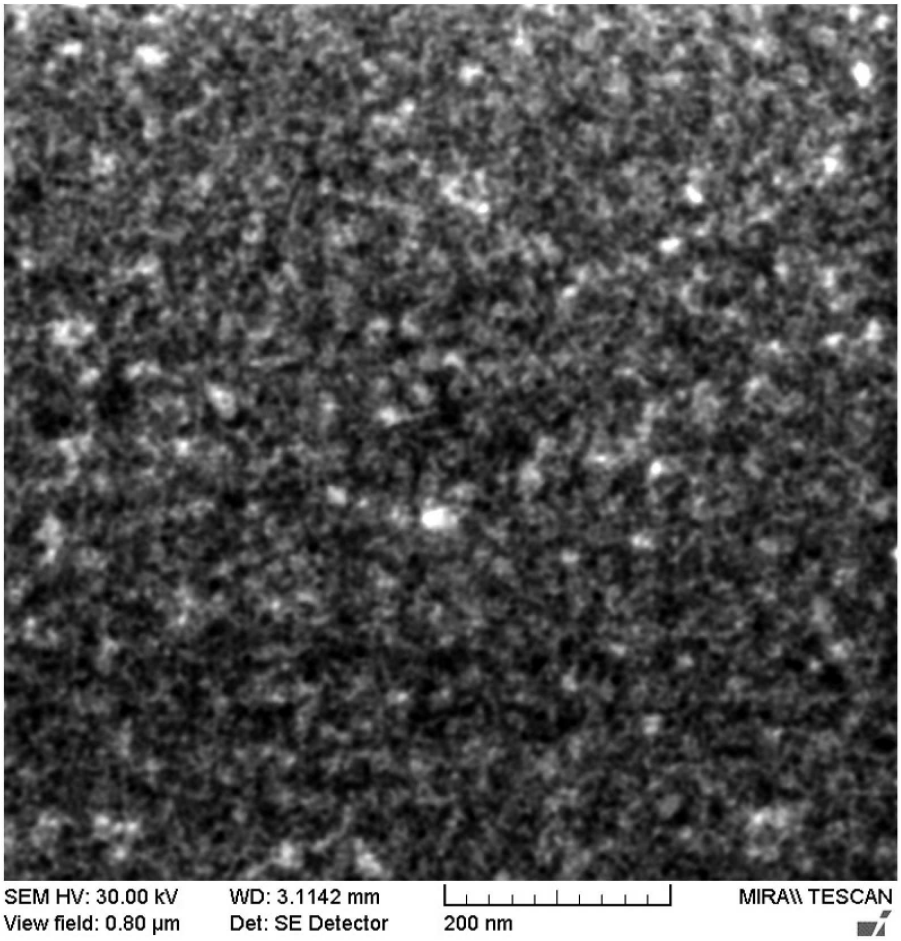

Image of the magnetron sputtered Pt-Sn-cerium oxide film: (a) SEM
149x144mm (600 x 600 DPI)

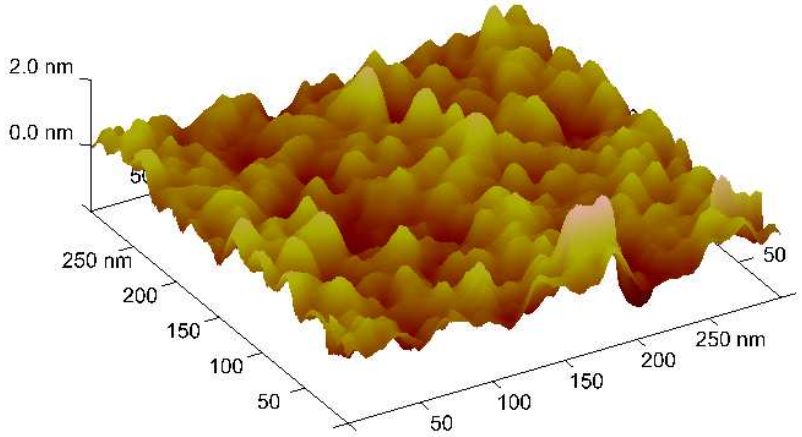

Image of the magnetron sputtered Pt-Sn-cerium oxide film:(b)AFM

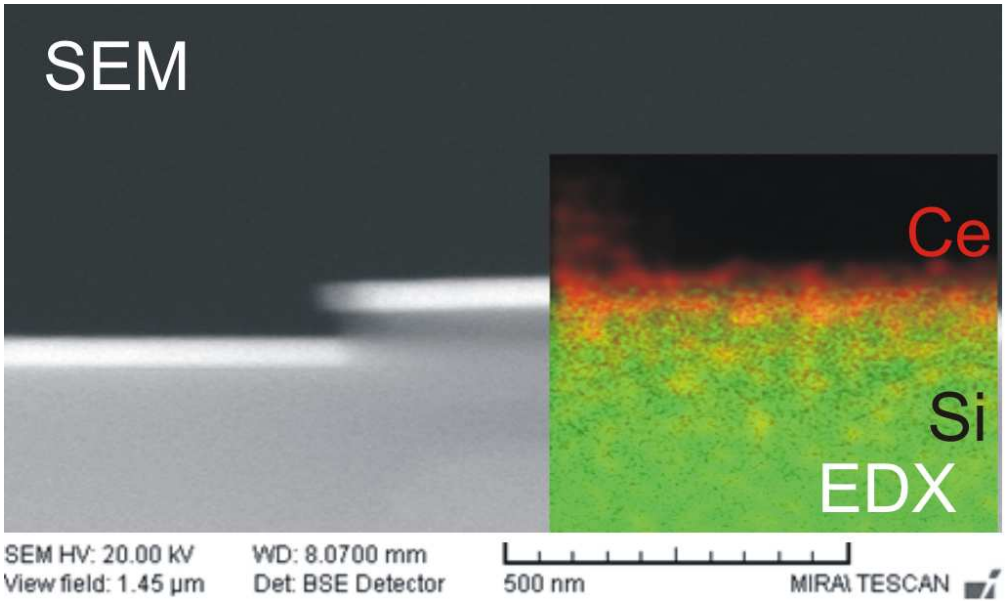

Cross-sectional SEM and EDX image of the Pt-CeO2/Si catalyst film.
43x25mm (600 x 600 DPI)

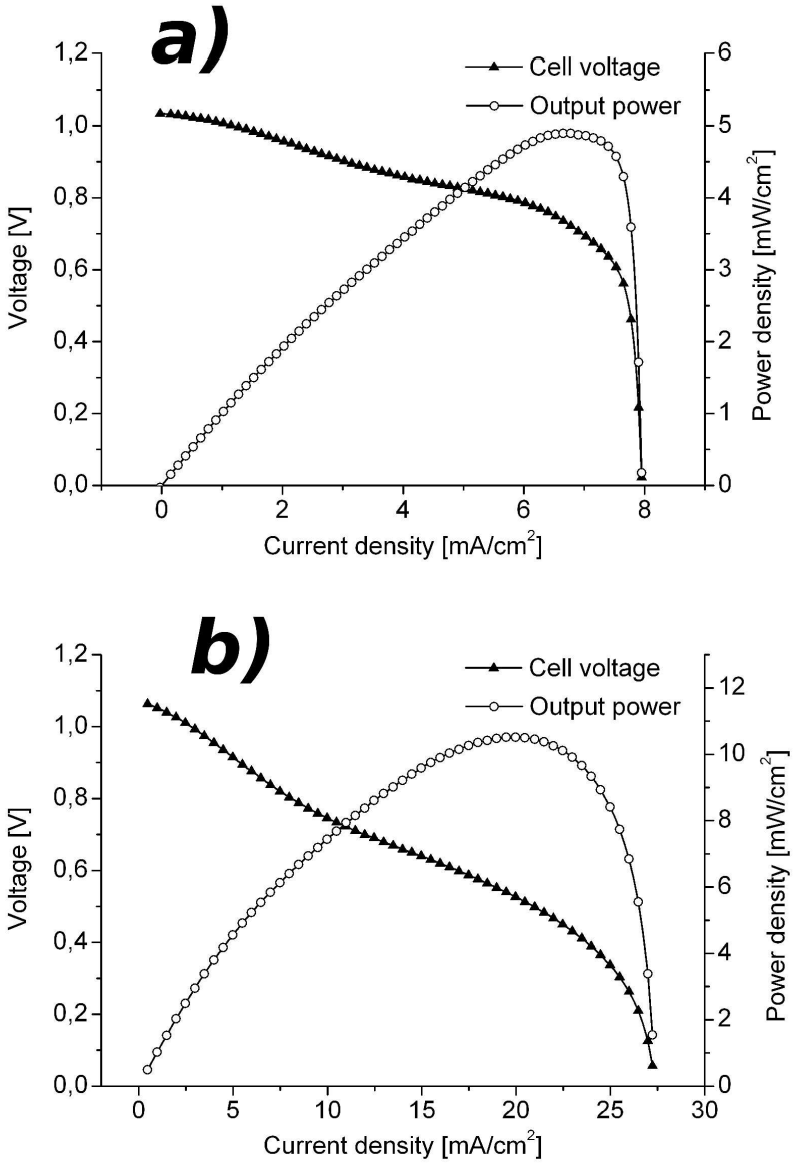

Polarization and power density vs. current density using hydrogen/air flow at room temperature. FC with (a) Pt-CeO2 anode, (b) Pt-Sn-CeO2 anode

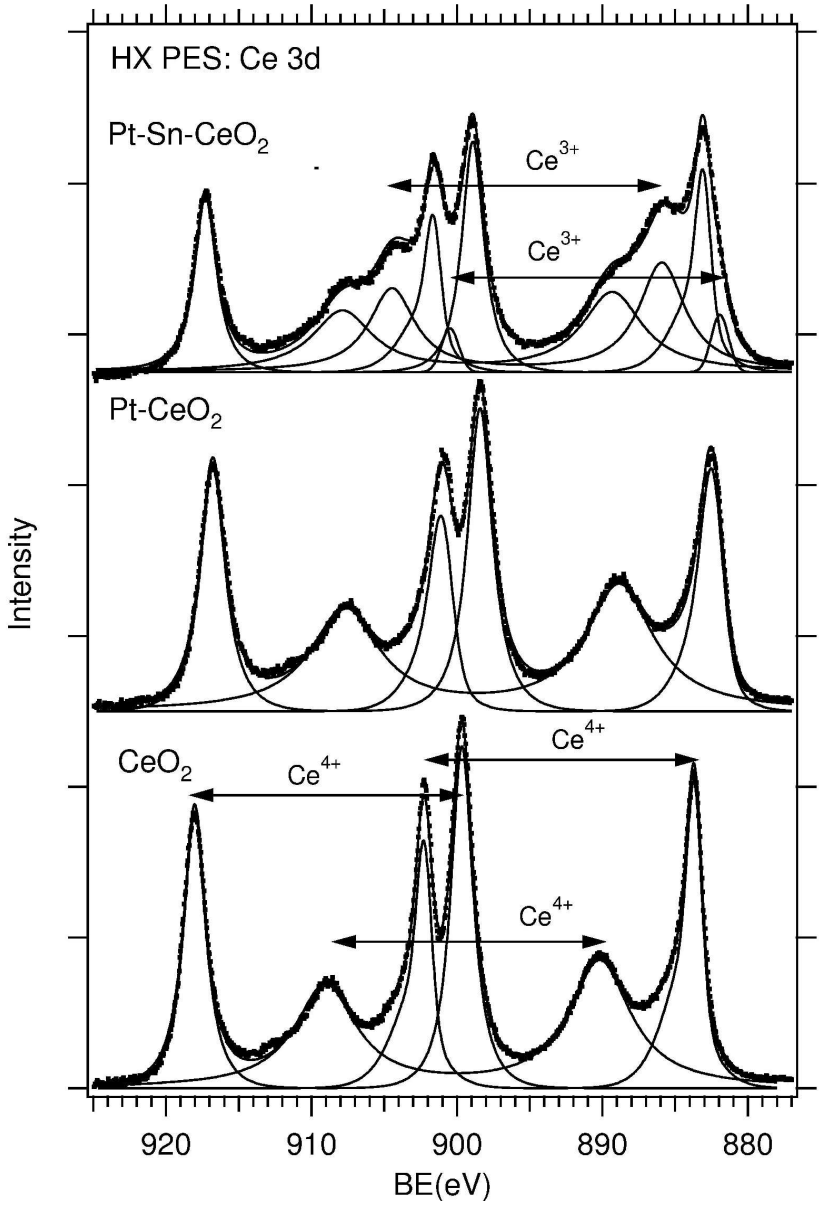

Ce 3d HX PES spectra (hν = 5946.8 eV) of the rf magnetron sputtered films. Bottom spectrum was measured on pure cerium oxide film, upper spectra on Pt and Pt-Sn doped samples.
156x192mm (600 x 600 DPI)

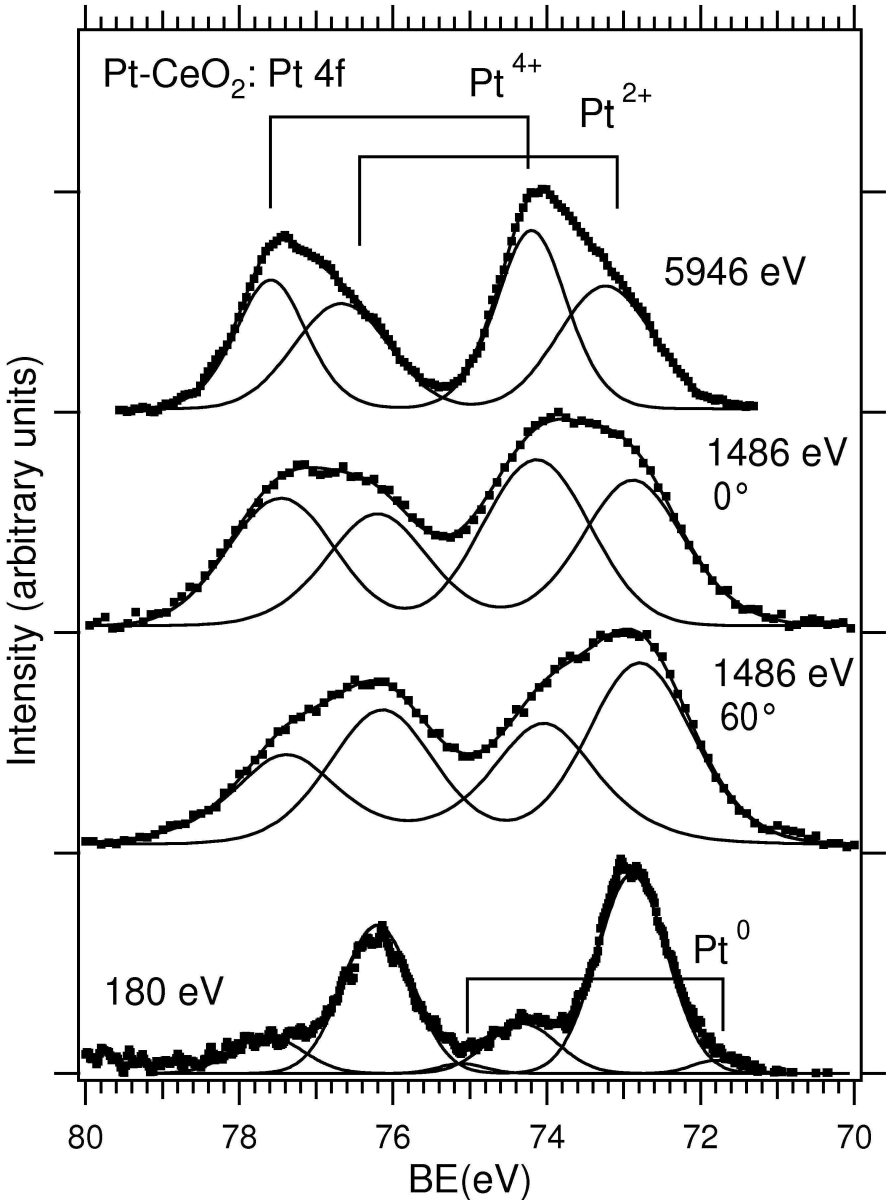

The SX, XPS at photoemission angle of 20° and 60°, and HX Pt 4f spectra of the Pt-CeO2 film.
124x153mm (600 x 600 DPI)

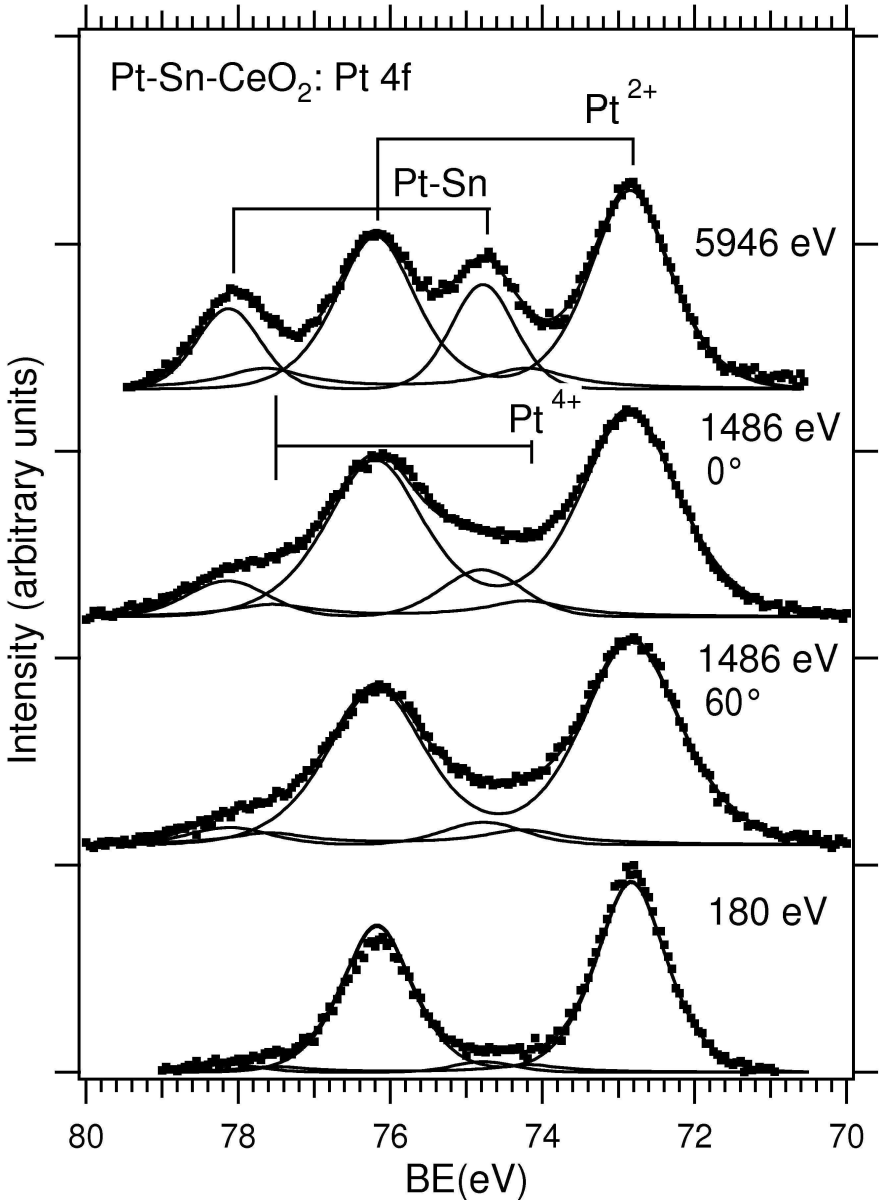

The SX, XPS at photoemission angle of 20° and 60°, and HX Pt 4f spectra of the Pt-Sn-CeO2 film.
124x153mm (600 x 600 DPI)

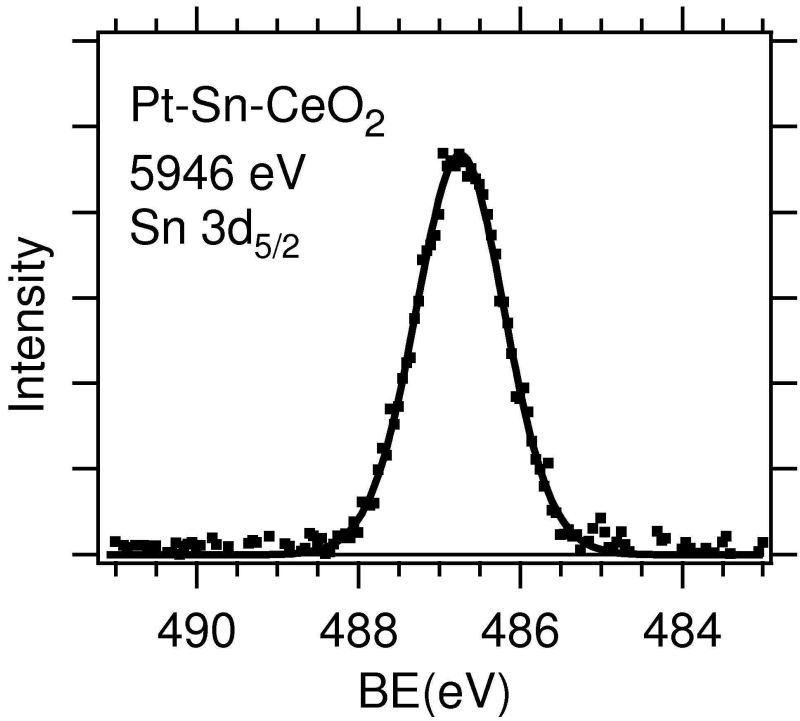

The HX Sn 3d5/2 spectra of the Pt-Sn-CeO2 film.
102x73mm (600 x 600 DPI)

Table 1. The relative concentrations of Pt^{4+} and Pt^{2+}

	Pt^{4+}/Pt^{2+}	$Pt(Sn)/Pt^{2+}$
180 eV	0.24	0.12
1486 eV 60°	0.77	0.15
1486 eV 20°	1.06	0.26
5946 eV	1.45	0.6